SDÜ FEN-EDEBIYAT FAKÜLTESİ SOSYAL BİLİMLER DERGİSİ, AĞUSTOS 2018, SAYI: 44, SS. 1-13

SDU FACULTY OF ARTS AND SCIENCES JOURNAL OF SOCIAL SCIENCES, AUGUST 2018, NO: 44, PP. 1-13.

Evaluation of Industrialization Effects on Urbanization and Heat Island Formation Using Remote Sensing Technologies: A Case of Istanbul Bağcılar District[1]

GULCAN SARP*, KADIR TEMURCIN, YOLCU ALDIRMAZ

Süleyman Demirel University, Faculty of Arts & Sciences, Department of Geography, 32260, Isparta, Turkey
gulcansarp@sdu.edu.tr, Telephone: +90 246 211 4332

Abstract: The new industrial labor opportunities started in the 1980s in Istanbul Bağcılar district caused a population shift from the countryside to the cities. Depending on the increase in urbanization, urban energy consumption causes urban heat island (UHI) formation in the region by changing local heat models. In this study, the spatial and temporal effects of industrialization on urbanization and heat island formation in Istanbul Bağcılar district for 1980-2000 and 2015 years were examined. According to results, in the region, UHIs distribution over the years changed based on the industrial locations and urbanization pattern. In densely built-up and industrial areas, UHIs distribution slightly differs from other sparsely distributed built-up areas due to the spectral response of constructed surfaces in the heat range of the electromagnetic spectrum. UHI mainly clustered in the western, northeastern and central part of the region where the densities of built-up areas are high. In the region, from 1986 to 2015 the UHI effects in the western, northeastern and central part of the region increased not only depend on the increase in urbanization and industrialization but also depend on industrial relocation.

Keywords: Urban heat island, Normalized built-up difference index, Relocation analysis, Industrialization, Urbanization

Introduction

The urban heat island (UHI) effect can be defined as higher urban temperature values when compared with surrounding rural areas (OKE, 1982). The change in land coverings due to urbanization is a major effect to UHI, such as buildings and some industrial activity of urban areas causes the areas to heat up (DU, et al. 2009; LIU and ZHANG, 2011; EL-NAHRY and RASHASH, 2013). Urban areas are dominated by built-up lands, and therefore the conversion of natural lands into built-up lands effects on local climate which can result in the UHI effect (XU, 2007). Urbanization also adversely influences the regional weather and climate (LANDSBERG, 1981). The UHI effect can vary depending on the size of the urban area, types, and density of buildings, and land use and land cover type etc. If the relationship between urban area and the amount of the UHI were known, it would be possible to identify thermally effective models of urban development (LINDA and OLUWATOLA, 2015).

The study of urban spatial growth and the resulting UHIs requires accurate and high spatial resolution data on urban built-up areas. Built-up mapping for urban can be used as an indicator of urban growth over the times (WENG, 2008). Recent advances in the remote sensing analysis technologies and presence of archived satellite imagery and aerial photographs enable to analyze temporal, spatial development on industrialization and effects of industrialization not only on rapid urbanization but also heat island formation. Remotely sensed data derived indices successfully used to map the built-up in urban areas, such as the Urban Index (UI) (KAWAMURA et al., 1996), Normalised Difference Built-up Index (NDBI) (ZHA et al., 2003), and Index-based Built-up Index (IBI) (XU, 2008) have been applied in several studies for built-up mapping. For many studies, it is very important to have access to reliable approximations of land surface temperature (LST) along the large spatial and temporal scales. Early in 1833, the concept of UHIs was described by Luke Howard (HOWARD, 1833), and since then numerous studies have been made on this research topic. UHI mainly appeared in the clustered distribution of LST, which is noticeably affected by urbanization (DOUSSET and GOURMELON, 2003; SUN et al., 2010). Earlier studies have shown that the higher the urban intensity or imperviousness, usually the higher the LST. Therefore, analyzing the relationship between the LST and the built-up area provides an alternative for studies of urban grown and related surface UHIs phenomena (OKE, 1976; WENG, 2001). Since the 1960s, with the advent of remote sensing technology, image taken from Thermal Infra-Red (TIR) region

[1] **Acknowledgments:** This study was financially supported by the Scientific Research Projects Coordination Unit of Suleyman Demirel University (SDU), Turkey. Project No. SDU BAP, 4972-GUP-17. We would also like to thank the General Command of Mapping, Turkey for providing orthophoto data free of charge under the project.

of the electromagnetic spectrum has been extensively employed to measure LST and afford basic data for the UHIs analysis. Comparing the traditional meteorological methods, remote sensing technology has the benefits of high-resolution and wide-coverage of numerous continuous sampling points (LIU and ZANG, 2011).

Bağcılar district of the Istanbul has a characteristic of industrialization in the last 30 years and the experience of intensive urbanization parallel to this (TEMURÇIN, 2013). The new industrial labor opportunities started in the 1980s in Istanbul Bağcılar district caused a population shift from the countryside to the cities. Because of this, urbanization in the province has been increasing rapidly since the 1980s. For that reasons, the determination of the relationship between the urban texture and the formation of UHIs in areas where urbanization has developed rapidly is of great importance for future urban planning in the Bağcılar district.

This article presents findings, the spatial and temporal effects of industrialization on urbanization and heat island formation in Istanbul Bağcılar district for 1980-2000 and 2015 years. Information about the industrial areas was obtained from the database of Istanbul Chamber of Industry. The geographical coordinates of industrial areas were determined using Google Earth and Istanbul city guide and then mapped in Geographic Information Systems (GIS) environment according to years of establishment. Urbanization information was gained from, Landsat-5 TM and Landsat 7-ETM images by using NDBI. For the mentioned years, heat island occurrences which are directly related to the urban intensity have been obtained from TIR bands of Landsat-5 TM and Landsat 7-ETM satellite images.

Description of the Study Area

The study area is the Bağcılar district of Istanbul, an area is approximately 22 km². Bağcılar district is one of the most densely populated, urbanized and industrialized districts of the Istanbul where the temporal and spatial effects of industrialization are intensively monitored (Fig. 1-a).

Rapid urbanization and demand for denser constructions in the Bağcılar region caused by the industrialization started in the 1980s. The industrial establishments in the region have chosen the main roadsides and immediate neighborhoods as the establishment places (Fig. 1-b).

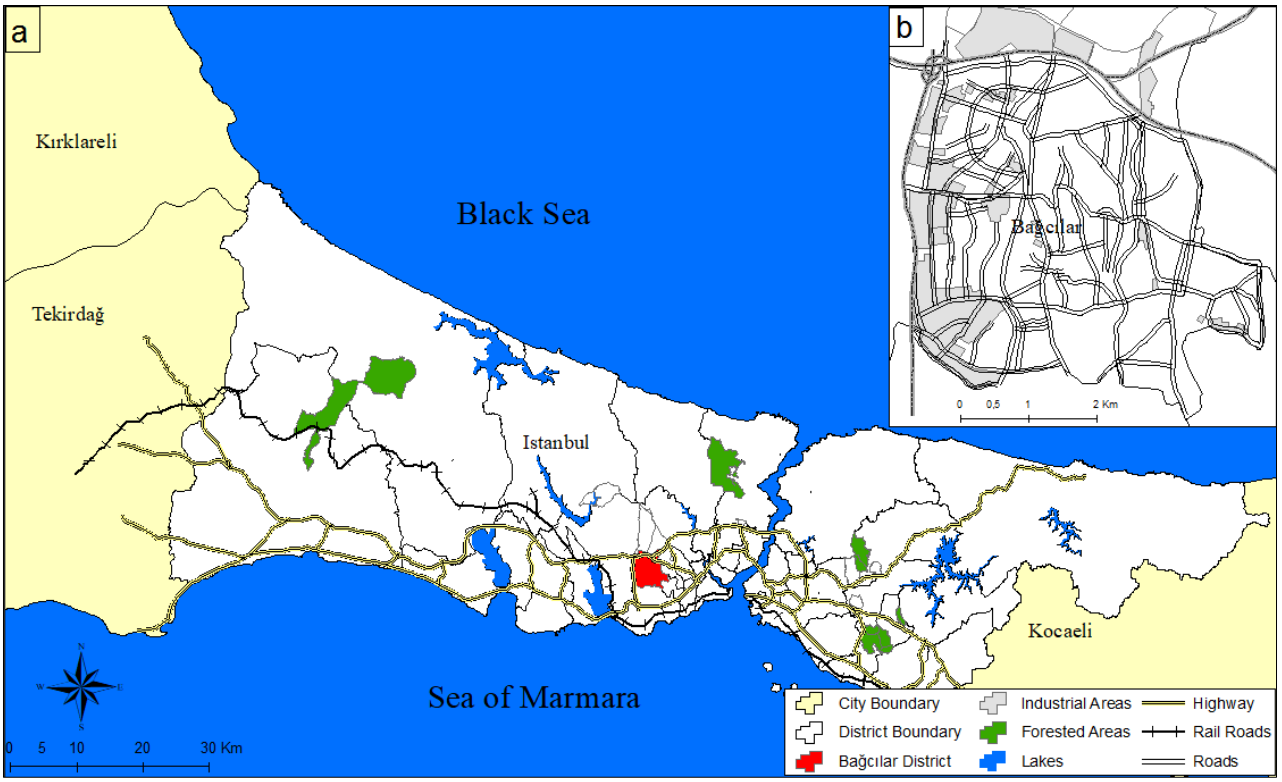

Figure 1: Location Map of the Study area

Data

The satellite data used in this study are Landsat-7 Enhanced Thematic Mapper Plus (ETM+) image acquired on 19 August 2015, 10 August 2000 and Landsat-5 Thematic Mapper (TM) image 21 August 1986 (path 180, row 032, covering Bağcılar district. The images are cloud-free except 1986 Landsat 5 TM image. The Landsat TM and ETM data, which has TIR band, is one of the most extensively used remotely sensed data for LST retrieving because of its 30 to 120-meter spatial resolution and free accessibility from the US Geological Survey (USGS) website. The acquisition date, spectral and spatial properties of the image data are given in Table 1.

Table 1: The properties of the used satellite images

Satellite Type and Acquisition Date	**Bands**	**Wavelength (micrometers)**	**Resolution (meters)**
L-7 ETM (19-08-2015) L-7 ETM (10-08-2000)	Band 1 - Blue	0.45-0.52	30
	Band 2 - Green	0.52-0.60	30
	Band 3 - Red	0.63-0.69	30
	Band 4 - Near Infrared (NIR)	0.76-0.90	30
	Band 5 - Shortwave Infrared (SWIR) 1	1.55-1.75	30
	Band 6 - Thermal	10.40-12.50	60 * (30)
	Band 7 - Shortwave Infrared (SWIR) 2	2.08-2.35	30
	Band 8 - Panchromatic	.52-.90	15
L-5 TM (21-08-1986)	Band 1 - Blue	0.45-0.52	30
	Band 2 - Green	0.52-0.60	30
	Band 3 - Red	0.63-0.69	30
	Band 4 - Near Infrared (NIR)	0.76-0.90	30
	Band 5 - Shortwave Infrared (SWIR) 1	1.55-1.75	30
	Band 6 - Thermal	10.40-12.50	120** (30)
	Band 7 - Shortwave Infrared (SWIR) 2	2.08-2.35	30
* ETM+ TIR band is acquired at 60-meter resolution and resampled to 30-meter pixels. ** TM TIR band is acquired at 120-meter resolution and resampled to 30-meter pixels.			

Information about the industrial areas for each year was obtained from the database of Istanbul Chamber of Industry which includes the address establishment data and type of the industry etc. (Fig. 2) and their geographic coordinates were collected from the city map of the Istanbul Metropolitan Municipality and Google Earth. Locations of industrial and built-up areas were verified by field check and high-resolution orthophotos belonging to 1986, 2003 and 2015 (Fig. 3).

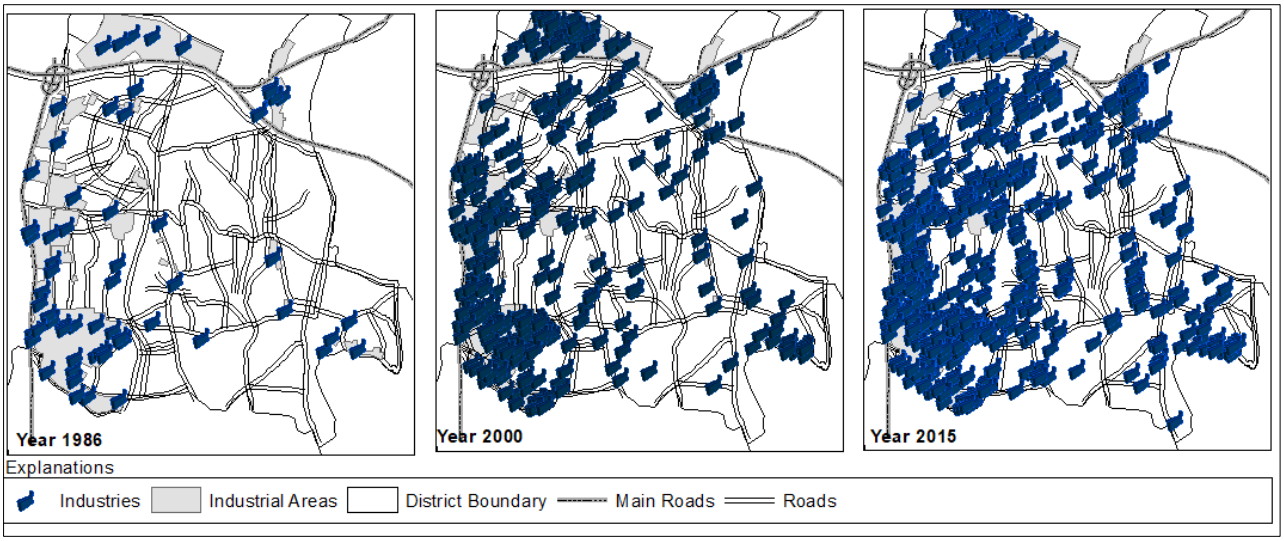

Figure 2: Spatial distribution of industries for the year 1986, 2000 and 2015

Figure 3: Sample orthophotos belonging to 1986, 2003 and 2015 years, field photos and ground control points (GCPs) measurement location used for accuracy analysis

Method of the Study

The method of this study composed of four different parts. In the first part, the land surface temperature is extracted from TIR bands of the Landsat-TM and Landsat ETM data. In the second part urban built-up areas extracted from SWIR and NIR bands of the satellite data by using NDBI. In the third part databases on industrial areas were established. In the final part, temporal and spatial relocation analysis of the industrial plants were carried out to investigate the formation and distribution of heat islands. The method of the study is summarized in the flowchart given in Fig. 4.

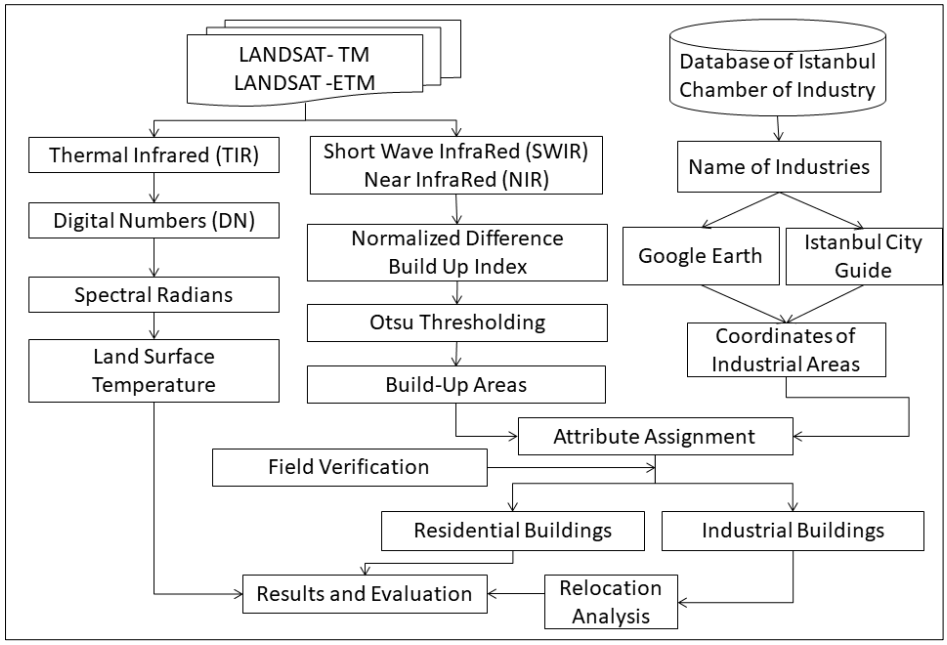

Figure 4: Flow chard of the Study

Land Surface Temperature Retrieval

The use of satellite measurements in the TIR seems to be very attractive since they can give access to global and unbiased approximations of LST (KERR, et al., 2004). Satellite TIR sensors measure a radiance, which can be translated into top-of-atmospheric (TOA) brightness temperature (KERR, et. al. 2004). The derivation of LST from satellite TIR bands requires several processing steps like sensor radiometric adjustments, atmospheric and surface emissivity corrections etc. In the study to derive LST from TIR data firstly the digital numbers recorded by the radiometer are converted into radiances by using equation (1)

$$L_\lambda = M_L Q_{cal} + A_L \quad (1)$$

where L_λ is TOA spectral radiance of sensor aperture, M_L is band specific multiplicative rescaling factor from the metadata, A_L is band specific additive rescaling factor from the metadata and Q_{cal} is the quantized and calibrated standard product pixel values.

After calculation of TOA spectral radiance brightness values, are converted to temperature values which in Kelvin by using the equation (2).

$$T = \frac{K_2}{\ln(\frac{K_1}{L_\lambda}+1)} \quad (2)$$

where T is the temperature in Kelvin (K) and K_1 and K_2 band specific thermal conversion constant from the metadata. For Landsat 5 and Landsat K1 and K2 constants are given in Table 2.

Table 2: Calibration constants of Landsat satellites (USGS, 2013)

	K1 666.09 W/(m2 sr µm)	**K2 W/(m2 sr µm)**
Landsat 5 TM	607.76	1260.56
Landsat 7 ETM+	666.09	1282.71

Urban Built-Up Area Detection

Urban built-up area extracted from remotely sensed data by using normalized NDBI. This index is used for the quickly and objectively extract to urban built-up areas where there is noticeably a higher reflectance in the SWIR region than the NIR region. The NDBI was mainly developed for Landsat TM sensors. But, it will work with any multispectral sensor with a SWIR band between 1.55-1.75 μm and a NIR band between 0.76-0.9 μm (ZHA et al., 2003). The formula of the NDBI is;

$$NDBI = \frac{(SWIR-NIR)}{(SWIR+NIR)} \quad (4)$$

NDBI values range between +1 to -1 high values correspond to built-up areas. On the other hand, values near to -1 correspond to other land use classes. Precise built-up region information can be gain by adjusting threshold values of NDBI. In the study, Otsu threshold is used to differentiate built-up areas from other land use classes. Otsu method automatically performs clustering-based image thresholding, or, the reduction of a gray level image to a binary image (OTSU, 1979).

Accuracy Assessment

The term accuracy refers to the maximum error to be expected in the values of a dataset. The accuracy of the NDBI is tested with high-resolution orthophotos and ground truth data at randomly selected 250 building locations. The ground truth data, which involves GCPs coordinates and high-resolution orthophotos, were compared with the resultant NDBI by using Binary Diagnostic Test in NCSS 11 Statistical Software (2016). The Binary Diagnostic Test measures are used to calculate, analyze, and compare the sensitivity and the specificity of the diagnostic tests, along with various other summary measures. The test includes calculation of True Positive (TP), True Negative (TN), False Positive (FP), and False Negative (FN) components by the comparison of ground truth data with the resultant binary image. TP (A) is the regions defined as a building both in the ground truth and in the resulted binary image. TN (C) is the regions that are not defined as a building in the ground truth and in the resultant binary image, respectively. FP (B) is the buildings that cannot be defined and FN (D) refers to the regions which are defined as buildings although they are not in the ground truth (SHUFELT et al., 1993). Based on these components the Sensitivity, Specificity, False Negative Rate, False Positive Rate, Positive Predictive Value, Negative Predictive Value, Prop. Correctly Classified, Prop. and Incorrectly Classified are calculated using the formulas;

Sensitivity	(TPR) A / (A + C)	(5)
Specificity	(TNR) D / (B + D)	(6)
False Negative Rate	C / (A + C)	(7)
False Positive Rate	B / (B + D)	(8)
Positive Predictive Value	(A / (A + B)	(9)
Negative Predictive Value	D / (C + D)	(10)
Prop. Correctly Classified	(A + D) / N	(11)
Prop. Incorrectly Classified	(B + C) / N	(12)

Results and Discussions

The intent of the data analysis is to model the relationship between urban expansion, industrial expansion, and net thermal emissions. To do so, a set of analysis models was constructed. In the study, land surface temperature was extracted from TIR band of the remotely sensed TM data set. LST data not only a measure of the degree of surface temperatures of the entire urban area but also the spatial extent of the surface UHIs effects (YUAN and BAUER, 2007) (Fig. 5). According to results the highest temperature variations at where the industrial zones are in the city. It was clearly seen that the factories in the Bağcılar industrial area might be considered as the main source of high heat and the most significant cause of UHIs in the city (CORUMLUOGLU and ASRI, 2015).

In 1986, when urbanization started due to industrialization, the mean temperatures in the urban and industrial areas are 17,99 ^{0}C and 17.31 ^{0}C, respectively. However, in 2000 these mean values drastically increase to 24,84 ^{0}C and 25,24 ^{0}C, respectively. This change was due chiefly to the industrial and urban extension with a consequent change in the ratio of sensible heat flux to latent heat flux. When came in 2015 slight increase in temperature is observed in the industrial (25,93 ^{0}C) and urban areas (25,98 ^{0}C). In this year some industrial facilities were relocated to other areas outside the municipal borders (Fig. 8 a, b, c). The shifts in industrial plants also caused some changes in heat island distribution over the area. With the expansion of urban area, the distribution of UHIs in 2000 and 2015 was greater than 1986. The increase in UHIs was consistent with the new urban areas developed since 1986.

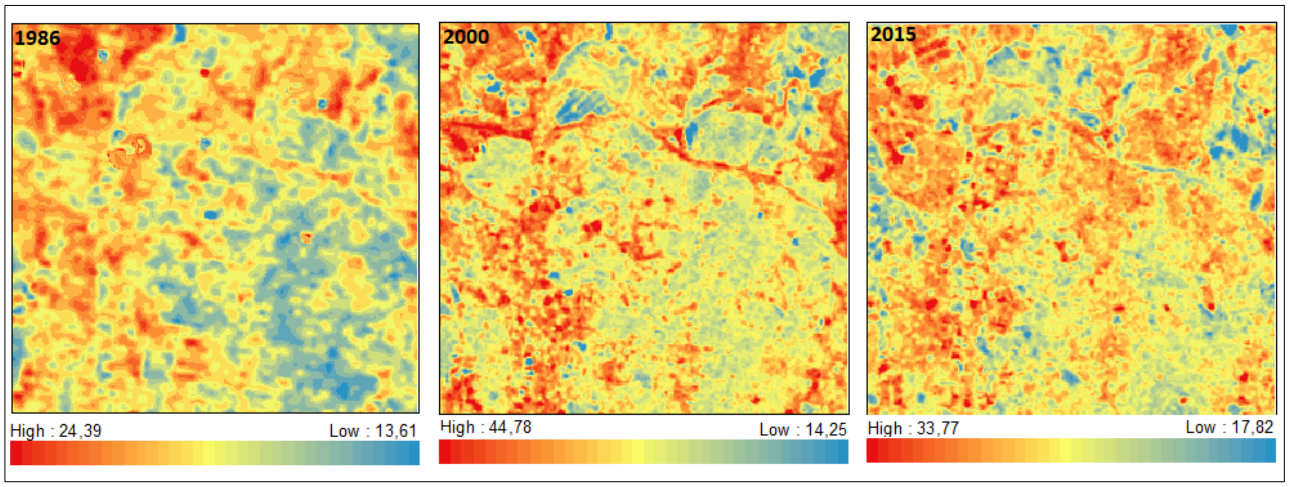

Figure 5: The Distribution of Urban Heat Islands over the Bağcılar District

Table 3: Surface temperature (^{0}C) by land-cover type

		L-5 TM (21-08-1986)	L-7 ETM (10-08-2000)	L-7 ETM (19-08-2015)
Urban	Min	16,39	23,68	24,16
	Max	20,46	28,37	29,28
	Mean	17,99	24,84	25,93
	Std	0,70	0,75	0,85
Industrial	Min	17,31	19,80	23,21
	Max	20,90	29,28	31,10
	Mean	18,91	25,24	25,98
	Std	0,71	1,76	1,33

NDBI-Derived Result and its Accuracy

The urban built-up lands were extracted from the NDBI image by using Otsu thresholding under the assumption that a positive value of NDBI should indicate built-up areas (Fig. 6). According to NDBI results, in 1986 there are 13646 built-up pixels, in 2000 there are 56023 built-up pixels, in 2015 and there are 62627 built-up pixels constitutes nearly 18%, 72% and 82% of the entire study area, respectively.

The accuracy of the built-up areas was tested with the finer resolution orthophotos and field test. The GCPs were collected from randomly selected 250 points Fig. 3. The extracted NDBI binary images were overlaid on the orthophotos after image to image registration, and then visually inspected pixel by pixel. All resultant binary-images were assessed using the same points. The point-based performance evaluation results are given in Table 4. The results of the accuracy assessment show that the algorithm provides Sensitivity for 1986, 2000 and 2015 NBBI are 0.81, 0.88 and 0.91, respectively. On the other hand, specificity for 1986, 2000 and 2015 NBBI are 0.39, 0.4118 and 0.33, respectively. The proportion of Correctly Classified for 1986, 2000 and 2015 NBBI are 0.62, 0.72 and 0.74, respectively. This indicates the success of the Otsu thresholding applied NDBI based build up area technique.

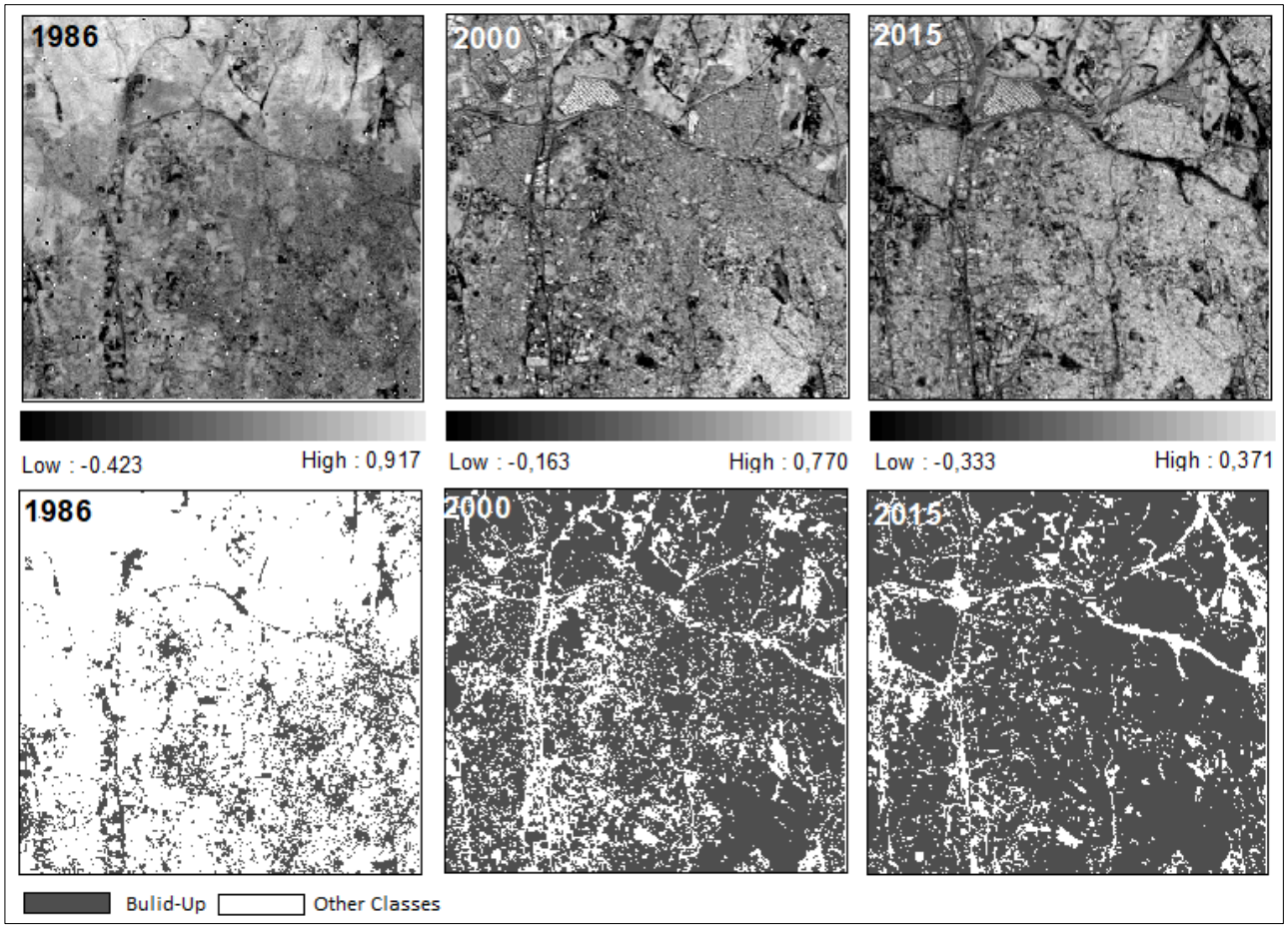

Figure 6: NDBI (above) and Otsu threshold applied NDBI (Below) for the years of 1986, 2000 and 2015

Table 4: Diagnostic test result rates of point-based performance evaluation

	NDBI (21-08-1986)	NDBI (10-08-2000)	NDBI (19-08-2015)
TP (A)	110	150	160
FP (B)	70	50	50
TN (C)	25	20	15
FN (D)	45	35	25
Sensitivity (TPR) A / (A + C)	0.81	0.88	0.91
Specificity (TNR) D / (B + D)	0.39	0.41	0.33
False Negative Rate C / (A + C)	0.18	0.11	0.08
False Positive Rate B / (B + D)	0.60	0.58	0.66
Positive Predictive Value (A / (A + B)	0.61	0.75	0.76
Negative Predictive Value D / (C + D)	0.64	0.60	0.62
Prop. Correctly Classified (A + D) / N	0.62	0.72	0.74
Prop. Incorrectly Classified (B + C) / N	0.38	0.27	0.26

To find out the change of the built-up areas from 1986 to 2000 and 2000 to 2015, the Otsu threshold applied two binary images were overlaid to obtain a difference image by subtracting matching pixels. The difference image showed the negative, positive and no-change area in the 14 and 15 years (Fig. 7). According to results from 1986 to 2000 62,46 % positive and 7,27% negative change was observed. On the other hand, from 2000 to 2015 16.84% positive change and 8,24% negative change were observed in the area (Table 5). In these figures, positive changes and no-change areas mostly correspond to new and previously built-up areas, respectively.

It should be emphasized that the determination of the accuracy of land surface temperature (LST) from the Landsat TIR bands is outside the scope of this study. In the study, the comparison of land surface temperature has been made using three Landsat data sets. These years were used to indicate relative spatial and local

variations in the temperature. The comparison of land surface temperature was made not only using the same data sets but also the same wavelength interval data. The comparison of spatial change maps and UHIs shows that from 2000 to 2015 and from 1986 to 2000 years LST decreases in the negative change areas. However, from 2000 to 2015 and from 1986 to 2000 years LST increases in the positive change.

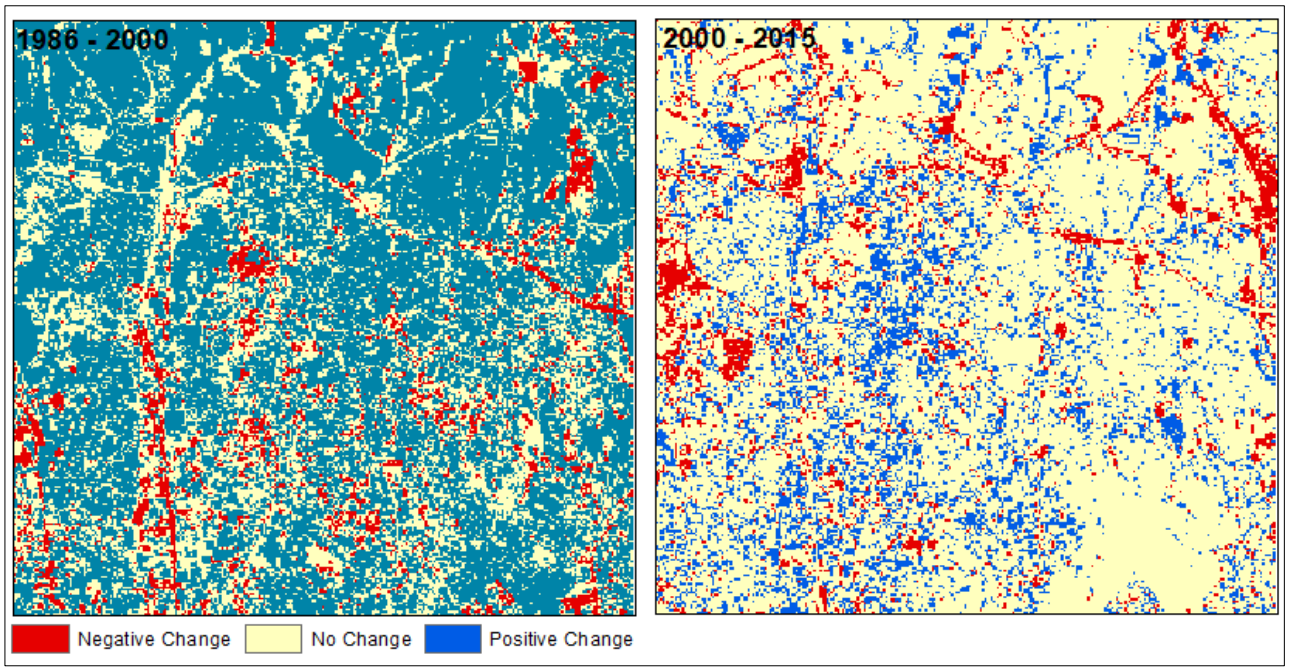

Figure 7: Spatial change map showing negative, positive and non-change patterns from 1986 to 2000 and 2000 to 2015

Table 5: Change matrix from 1986 to 2000 and 2000 to 2015

Land Cover Change	1986 to 2000 (%)	2000 to 2015 (%)
Negative Change	7,27	8,24
Non-Change	30,27	74,91
Positive Change	62,46	16,84

The spatial location of the industry in the urban space varies depending on the size of the industry, its connection to the market, what it produces, the sector, the sub-sector, and in what industry. From this point of view, the location of the industry in the city can be explained by the interaction of not only one factor but also more than one element. The most important factor here is that the factors are constantly changing according to time and place (TÜMERTEKIN, 1972; TEMURÇIN and ALDIRMAZ 2017 a, b; TEKELI, 1975, 2011).

From 1986 to 2015, industrialization and, accordingly, urbanization has rapidly developed in Bağcılar district (Fig. 2 and Fig.6, respectively). Up to1986 industrialization was located close to the main roads in the northern and western part of the Bağcılar district. Until that time urbanization rate was very low and it began to spreads around these industrial sites. When it came to the year 2000, industrialization threw the concentration in the northern and western parts of the district and continued its spread towards the district center. Parallel to these increase of the industrialization, the urbanization also has rapidly increased in the district. In 2015, industrialization has covered the northern and western parts of the province to a large extent and has increased the density in the district center and east of the district. Due to this rapid increase in industrialization, in 2015 urbanization in the province has reached its maximum level and vegetated and vacant areas reached its lowest level in the district.

According to the new arrangement made by the municipality in 2011, the establishment of large industrial enterprises in the city center was banned and the transfer of large industrial enterprises outside the city was encouraged. In this context, it was decided to move the large industrial sites and industrial enterprises located in the residential areas out of the residential areas and to move the industrial enterprises operating outside the

planned industrial areas to the planned industrial areas. According to these new regulations, many large industrial sites of 20-100 km have been moved out of the city. According to the relocation analysis, the most displacements in the industrial facilities were found within 20 km area (Fig. 8-a). On the other hand, many small industrial plants have moved to more convenient places in the city. These spatial displacements in the industrial facilities were obtained by using the industrial databases, including address information and activity status of the industrial facilities, provided by the Bağcılar district.

The displacement map of large industrial enterprises moving out of the district borders and displacement map of small industrial enterprises moving in and into the city is given in Fig. 8. a-b- c. As given Fig. 8-a, many industries shift out of the district borders in the east-west direction within the 20 km. By comparison of land surface temperature map with industrial displacement map from 2007 to 2017 reveals that land surface temperature decreased in the north, southwest and east part of the region due to the displacement of the industrial sites.

According to Fig. 8-b, some of the small industries shifted from outside the municipal borders to the Bağcılar district borders mostly in the north-west and south-east direction. By comparison of a land surface temperature map of 2000 and 2015 with industrial displacement map from 2007 to 2017 reveals that land surface temperature increased in the north and southwest part of the region due to the shift of the industrial sites inside district boundaries.

As shown in Fig. 8-c, some of the industries shifted inside district borders mostly in the north-west and south-east direction. By comparison of a land surface temperature map of 2000 and 2015 with industrial displacement map from 2007 to 2017 reveals that this relocation causes land surface temperature slightly increase especially in the southwest part of the region.

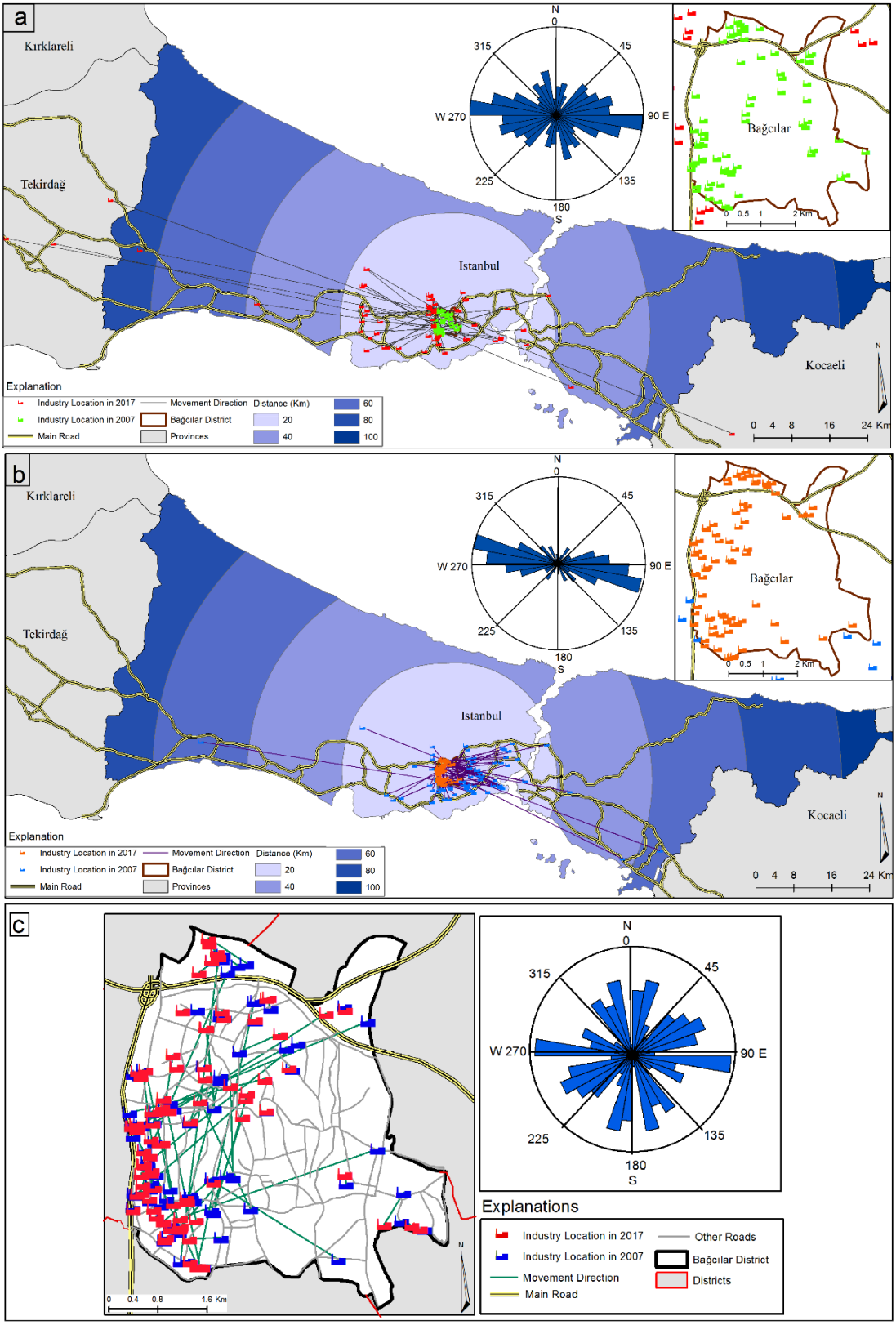

Figure 8: Relocation map of the industries (a) shifted to outside the Bağcılar district boundaries, (b) industries shifted from outside the district boundaries to the Bağcılar district boundaries, (c) shifted inside the Bağcılar district boundaries.

Conclusion

Rapid urbanization in Bağcılar district from 1986 to 2015 causes industrial production under big pressure in the district. These conditions provide for short-term spatial shifts in the industry. While local shifts of industry do not have much effect on the process of urbanization and the formation of heat island, shifts to other neighborhoods, provinces or out of provinces cause the new sites of the industry to enter a new mold in terms of urbanization and heat island formation. Depending on the changes in industrial locations especially, along with the transport of large industrial plants out of the city, significant changes have been observed in the spatial distribution of local heat islands in the Bağcılar district. On the other hand, displacements within and towards the district caused to increase heat islands, especially in industrialized areas. Unless the severe precautions are taken into consideration, rapid urban and industrial sprawl in Bağcılar will likely expand and the UHI effect will become more severe.

References

ARNOLD, C.L., GIBBONS, C.J. 1996. Impervious surface coverage: The emergence of a key environmental indicator Journal of the American Planning Association, 62 (2): 243-258.

CORUMLUOGLU, O, ASRI, İ. 2015. The effect of urban heat island on Izmir's city ecosystem and climate. Environmental Science and Pollution Research, Vol. 22, Issue 5, pp 3202–3211

DOUSSET, B.; GOURMELON, F. 2003. Satellite multi-sensor data analysis of urban surface temperatures and landcover. ISPRS J. Photogram. Remote Sens. 58: 43–54.

DU, M., WANG, Q., & CAI, G. 2009. Temporal and spatial variations of urban heat island effect in Beijing using ASTER and TM data. In Urban Remote Sensing Event, 2009 Joint (pp. 1-5). IEEE.

EL-NAHRY AH, RASHASH A. 2013. Impact of industrial areas on surface temperature using thermal infrared remote sensing and GIS techniques a case study of Jubail City, KSA. Dammam, Eastern Province, Saudi Arabia: The Eight National GIS Symposium in Saudi Arabia.

HOWARD, L. 1833. Climate of London deduced from meteorological observations. 3rd ed. Harvery and Darton, London.

KAWAMURA, M., JAYAMANA. S., TSUJIKO, Y. 1996. Relation between Social and Environmental Conditions in Colombo Sri Lanka and the Urban Index Estimated By Satellite Remote Sensing Data. International Archieve of Photogrammetry and Remote Sensing. 31 (Part-B7) 321-326.

KERR, Y. H., LAGOUARDE, J. P., NERRY, F., OTTLÉ, C. 2004. Land surface temperature retrieval techniques and applications: case of AVHRR. In: Thermal Remote Sensing in Land Surface Processes, D. A. Quattrochi y J. C. Luvall (eds), CRC Press, Florida, USA, pp. 33-109.

LANDSBERG, H.E. 1981. The Urban Climate; Academic Press: New York, NY, USA, pp. 84–89.

LINDA, A., OLUWATOLA, A. 2015. Impact of Landuse Change on Surface Temperature in Ibadan, Nigeria. International Journal of Environmental, Chemical, Ecological, Geological and Geophysical Engineering 9 (3): 235-241.

LIU, L., ZHANG, Y. 2011. Urban Heat Island Analysis Using the Landsat TM Data and ASTER Data: A Case Study in Hong Kong, Remote Sens. 3(7): 1535-1552.

Montanaro M, Gerace A, Lunsford A, Reuter D (2014) Stray Light Artifacts in Imagery from the Landsat 8 Thermal Infrared Sensor. Remote Sens. 6(11): 10435-10456. https://doi.org/10.3390/rs61110435

NCSS 11 STATISTICAL SOFTWARE, 2016. NCSS, LLC. Kaysville, Utah, USA, ncss.com/software/ncss.

OKE T.R. 1976. City size and the urban heat island Atmospheric Environment, 7: 769-779.

OKE, T.R. 1982. The energetic basis of the urban heat island. Quarterly Journal of the Royal Meteorological Society 108: 1-24.

OTSU, N. 1970. A Threshold Selection Method from Gray-Level Histograms, IEEE Transactions on Systems, Man, and Cybernetics, 9, 1: 62-66.

SHUFELT A.A., MCKEOWN D.M. 1993. Fusion of Monocular Cues to Detect Man-Made Structures in Aerial Imagery. CVGIP: Image Understanding, 57 (3): 307-330.

STANKOWSKI, S.J., 1972. Population Density as an Indirect Indicator of Urban and Suburban Land-Surface Modifications, U.S. Geological Survey Professional Paper 800-B, Reston, Virginia, pp. B219–B224.

SUN, Q., TAN, J., XU, Y. 2010. An ERDAS image processing method for retrieving LST and describing urban heat evolution: A case study in the Pearl River Delta Region in South China. Environ. Earth Sci. 59: 1047–1055.

TEKELI, İ. 1975. Endüstrinin Arazi Kullanımı Kararlarında Etken Olan Kurumsal Çerçeve. Peyzaj Mimarlığı, 49-55. (In Turkish)

TEKELI, İ. 2011. Kent, Kentli Hakları, Kentleşme ve Kentsel Dönüşüm. Tarih Vakfı Yurt Yayınları, İstanbul. (In Turkish)

TEMURÇIN, K., 2013. The development and structure of industry in the disrict of Bağcılar (İstanbul), Bulletin of Geography-Socio Economic Series, 20: 95-111, Torun Poland.

TEMURÇIN, K., ALDIRMAZ, Y., 2017a. İstanbul İlinde Sanayi: Tarihsel Gelişim, Yapısal Değişim, Mekânsal Dönüşüm, Süleyman Demirel Üniversitesi Yayınları, Isparta. (In Turkish)

TEMURÇIN, K., ALDIRMAZ, Y., 2017b, İstanbul İlinde Tekstil, Dokuma ve Giyim Sanayi: Yapısı, Özellikleri ve Dağılışı, Pegem Akademi Yayınları, Ankara. (In Turkish)

TÜMERTEKIN, E. 1972. İstanbul Sanayinde Kuruluş Yeri. İ. Ü. Coğrafya Enstitüsü Yayınları, İstanbul. (In Turkish)

YUAN, F., BAUER, M., E. 2007. Comparison of impervious surface area and normalized difference vegetation index as indicators of surface urban heat island effects in Landsat imagery. Remote Sensing of Environment, Vol. 106, Issue 3, pp. 375-386.

WENG, Q. 2001. A remote sensing-GIS evaluation of urban expansion and its impact on surface temperature in the Zhujiang Delta, China International Journal of Remote Sensing, 22 (10): 1999-2014.

WENG, Q. 2008. Remote Sensing of Impervious Surfaces: An Overview. In Remote Sensing of Impervious Surfaces; Weng, Q., Ed.; CRC Press, Taylor & Francis Group: Boca Raton, FL, USA, 2008.

XU, H. 2007. Extraction of urban built-up land features from Landsat imagery using a thematic oriented index combination technique. Photogrammetric Engineering & Remote Sensing, 73 (12): 1381-1391.

XU, H. 2008. A new index for delineating built-up land features in satellite imagery. Int. J. Remote Sens., 29, 4269–4276.

ZHA, Y., GAO, Y. AND NI, S. 2003. Use of normalized difference built-up index in automatically mapping urban areas from TM imagery. International Journal of Remote Sensing, 24: 583–594.

Other References

Istanbul Chamber of Industry

Istanbul Metropolitan Municipality

USGS (https://www.usgs.gov/)